

## Original Research Article

# A highly efficient and sustainable synthesis of 1-[(1,3-thiazol-2-ylamino) methyl]-2-naphthols under solvent-free conditions using graphene oxide substituted ethane sulfonic acid catalyst

Samaneh Hamidi Zare, Maryam Sadat Ghorayshi Nejad, Ali Saberi, Esmael Rostami\* 

Department of Basic Sciences, Faculty of Chemistry, Payame Noor University, Tehran, Iran

### ARTICLE INFORMATION

Received: 21 July 2022

Received in revised: 11 August 2022

Accepted: 12 August 2022

Available online: 22 August 2022

DOI: 10.26655/AJNANOMAT.2022.3.4

### KEYWORDS

Graphene oxide

Ethane sulfonic acid catalyst

Synthesis

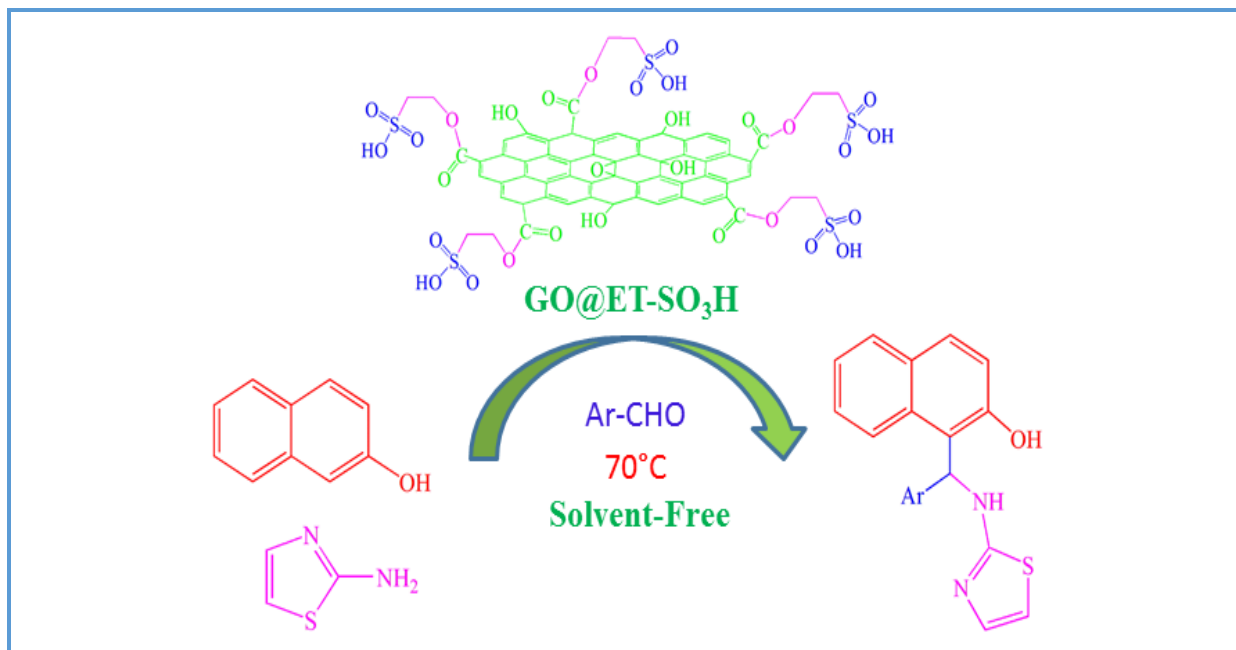
2-Aminothiazole

1-[(1,3-Thiazol-2-ylamino) methyl]-2-naphthols

### ABSTRACT

Graphene oxide functionalized by ethane sulfonic acid (GO@ET-SO<sub>3</sub>H) is an efficient and environmentally benign catalyst for the synthesis of 1-[(1,3-thiazol-2-ylamino) methyl]-2-naphthols. The synthesis was implemented through a one-pot process by using no solvent by the reaction of 2-naphthol, functionalized benzaldehydes, and 2-aminothiazol. First, graphene oxide was prepared according to a modified Hummers method. It was subsequently modified by 2-Hydroxyethyl disulfide, and then oxidized with performic acid to reach the catalyst (GO@ET-SO<sub>3</sub>H). The catalyst was characterized by X-ray diffraction (XRD), energy-dispersive X-ray spectroscopy (EDS), field emission scanning electron microscopy (FE-SEM), thermogravimetric analysis (TGA), and FT-IR spectroscopy. The catalyst exhibited efficient properties such as simple work-up, no byproducts, sustainability, nonmetal and safe components, stability under reaction conditions, and recoverability. © 2022 by SPC (Sami Publishing Company), Asian Journal of Nanoscience and Materials, Reproduction is permitted for noncommercial purposes.

## Graphical Abstract



## Introduction

Carbon-carbon bond formation has been widely studied in the synthesis processes. The Betti reaction [1] is one of the most important types of these reactions similar to the Mannich reaction [2]. 1-(Amino alkyl)-2-naphthols could be prepared from the Betti reaction known as the Betti bases. The Betti base derivatives are significant synthons and ligands in the asymmetric chemistry [3]. 1-(aminoalkyl)-2-naphthols are bioactive derivatives with antipain, antihypertensive, and antibacterial properties [4–6]. In fact, aminoalkyl naphthol can be originally prepared from the reaction of aldehyde, 2-naphthol and ammonia, or urea in ethanol for 9 to 36 hours. This method has some drawbacks including fast reaction rates and poor yields; making it inapplicable in a large scale production [7, 8]. Thus, a series of methodologies have been explored to prepare aminoalkyl naphthols through more efficient procedures (especially one-pot multicomponent reactions) to overcome the

drawbacks of classical synthetic routes [9–12]. The synthesis by using 2-naphthol, aldehydes, and amines has been performed by various catalytic systems including (+)-camphor-10-sulfonic acid [13], Fe<sub>3</sub>O<sub>4</sub>@SiO<sub>2</sub>-ZrCl<sub>2</sub>-MNPs [14], maltose [15], oxalic acid [16], ionic liquid [17], aragonite [18], NH<sub>3</sub>(CH<sub>2</sub>)<sub>5</sub>NH<sub>3</sub>BiCl<sub>5</sub> [19], and l-Valine [20]. However, these procedures and catalysts suffer from several drawbacks such as toxicity, long reaction time, vigorous conditions, tedious work-up, non-recoverability, and non-reproducibility.

Carbon-based catalysts are nontoxic and ecofriendly [21]. Thus, a series of catalytic systems were designed based on carbon [22]. Graphene and graphene oxide are two important allotropes of carbon functionalized to achieve desirable catalysts [23]. Graphene and graphene oxide-based structures have been employed in a large number of research projects [24].

The graphene structure encompasses benzene rings connected to each other [25]. In graphene, outer benzene ring converts into

functionalized carbon, showing catalytic activity. Functionalized graphene structures are similar to polynuclear aromatic rings with various functional groups and the chemistry is mainly originated from aromatic derivatives [26]. They are valuable compounds and a series of them can be found in natural sources; while a large number of these compounds have been prepared in the laboratory. Graphene and graphene oxide have exhibited various research features including catalysts, adsorbents, capacitors, nanocomposites, drug delivery, chemical, and industrial applications [27–29]. The synthesis of organic compounds was reported in a large number of publications with a series of procedures. However, the synthesis via sustainable processes by using green chemistry principles is the main synthetic procedure [30].

In this research, graphene oxide was functionalized by ethane sulfonic acid and employed as a catalyst to prepare 1-[(1,3-thiazol-2-ylamino) methyl]-2-naphthols under solvent-free conditions.

## Experimental

### *Materials and apparatus*

The applied chemicals were purchased from Merck and Iranian chemical companies. Thin-layer chromatography (TLC) was conducted by using silica gel 60 F<sub>254</sub> on aluminum plates. The melting points were determined through Thermal Scientific apparatus. XRD spectra were also obtained via PW1730 diffractometer. A SDT Q600 V20.9 Build 20 apparatus was utilized for thermogravimetric analysis (TGA). A BRUKER spectrometer was employed to record FT-IR spectra. Morphological assessments and elemental analyses were achieved by a scanning electron microscope (A Tescan Mira III, Czech) equipped with energy-dispersive X-ray spectroscopy (EDS or EDAX).

### *Preparation of single layer nanostructured graphene oxide*

The modified Hummers method was employed to prepare graphene oxide [31]. Concentrated sulfuric acid (100 mL) was poured into a 1000 mL round-bottomed flask immersed in an ice-water bath. Then, graphite (2 g) and NaNO<sub>3</sub> (2 g) were added to the flask. The mixture was stirred by a large magnet for 4 hours, and then potassium permanganate (6 g) was added in two portions at a time interval of 30 min. The mixture was stirred for 30 min in an ice bath. Subsequently, the ice-water bath was removed and the reaction was continued for 48 hours at room temperature. The mixture was diluted by slowly adding deionized water (200 mL) which warmed up the system. Stirring was further continued to reach the room temperature (2 hours). The mixture volume was again increased by deionized water (200 mL) and after 30 min, the oxidation was completed by hydrogen peroxide (10 mL). Upon the addition of hydrogen peroxide, the color turned yellow showing the reaction progress. After four hours of stirring, concentrated hydrochloric acid (HCl, 10 mL) was added and the mixture was stirred for another 60 min; the reaction was quenched and left at room temperature. After several hours, the graphite oxide precipitate settled down on the bottom of the flask. The solution volume on top of the precipitate was decreased to half by using a pipette and the mixture was centrifuged. The obtained precipitate (graphite oxide) was transferred to an Erlenmeyer flask and deionized water (100 mL) was added followed by 30 minutes of ultrasonication at room temperature. Finally, the new mixture (single layer nanostructured graphene oxide) was centrifuged and washed with deionized water, alcohol, and acetone. The final product was dried at room temperature.

### Preparation of catalyst (GO@ET-SO<sub>3</sub>H)

Dimethylformamide (DMF, 30 mL) was added to graphene oxide (1 g) and the mixture was sonicated for 30 min at room temperature. The obtained colloidal solution was charged with 2-Hydroxyethyl disulfide (3 mmol, 0.36 mL), triethylamine (0.70 mL), and dicyclohexylcarbodiimide (DCC, 3 mmol, 0.60 g). After 48 hours of stirring at room temperature, deionized water (5 mL) and dimethylsulfoxide (DMSO, 20 mL) were added and filtered hot. The resulting precipitates were washed with hot alcohol several times, deionized water, and acetone followed by drying at room temperature. In the next step, to precipitate (1 g) was added formic acid (30 mL) and sonicated for 30 min to afford a homogenized colloidal solution. Then, hydrogen peroxide (1 mL) was added and the reaction was continued for 24 hours. Finally, the crude precipitate was purified via centrifugation and washed efficiently with alcohol, deionized water, and acetone followed by drying at room temperature.

### General procedure for the synthesis of 1-[(1,3-Thiazol-2-ylamino) methyl]-2-naphthols by using the catalyst

Aromatic aldehyde (1 mmol) and catalyst (0.02 g, 0.007 mol % based on sulfonic acid by using EDAX results) were added to 2-naphthol (1 mmol, 0.14 g) and 2-aminothiazole (1 mmol, 0.10 g) and the mixture was homogenized by a glass rod. The mixture was heated in an oil bath. After completion of the reaction (TLC), acetone (5 mL) was added to the mixture and filtered hot. The catalyst was isolated as a precipitate on the filter paper and the mother liquor was recrystallized in acetone to afford the pure product. In the case of **4b**, the catalyst was used five times after recovery to examine its stability under the reaction conditions similar to the

above aldehyde, catalyst, 2-naphthol, and 2-aminothiazole portions.

## Results and Discussion

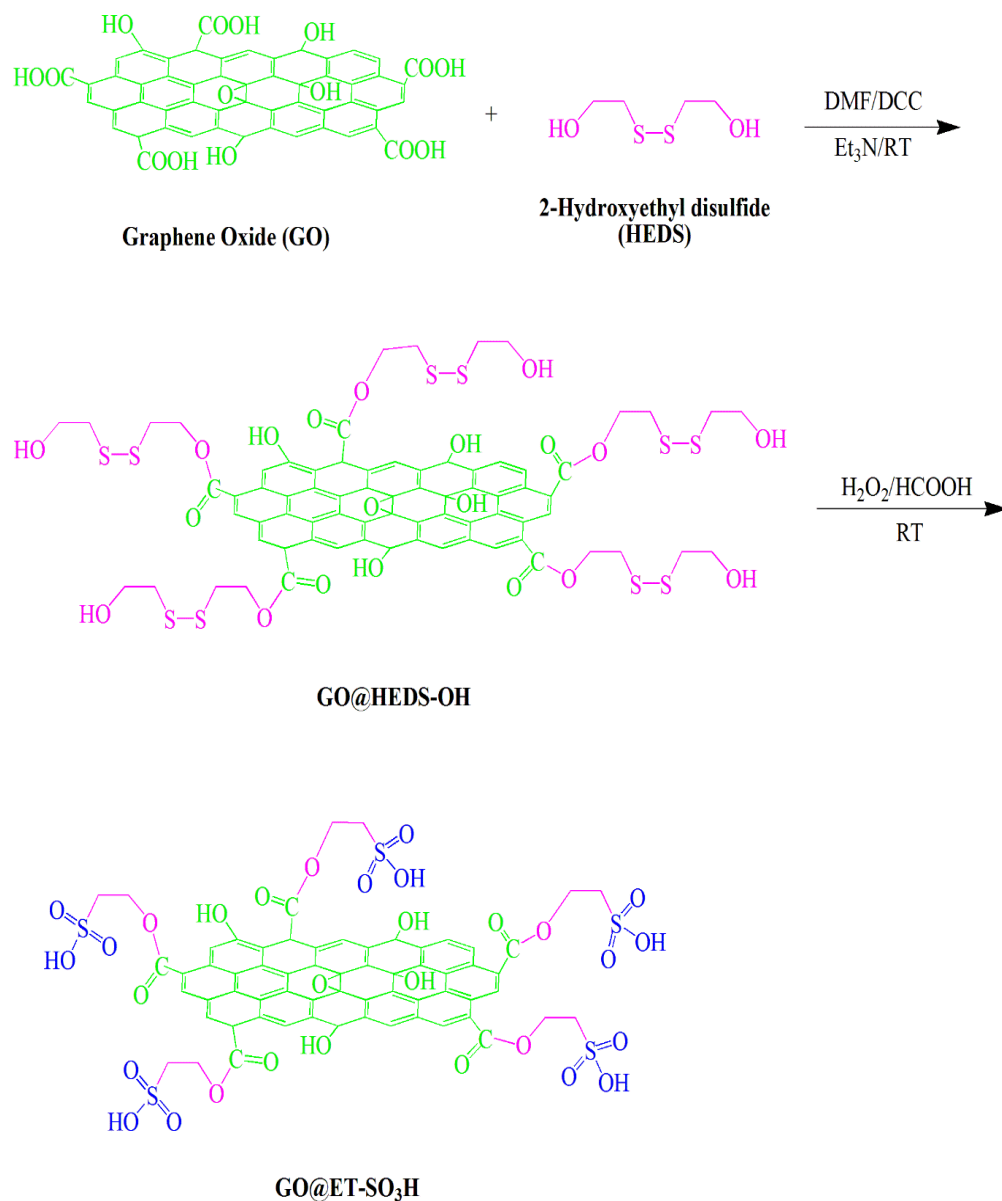
Graphene oxide was prepared by using the modified Hummers method from the oxidation of graphite in the presence of violent oxidants such as concentrated sulfuric acid, sodium nitrate, and potassium permanganate [31]. To prepare single-layer nanostructured graphene oxide, the resulting graphite oxide precipitate was treated in an ultrasonic bath. Graphene oxide functionalized with 2-Hydroxyethyl disulfide was prepared via ester formation in the presence of trimethylamine and DCC and the resulting product was treated with hydrogen peroxide in formic acid to afford the catalyst. The synthetic route for preparing catalyst from graphene oxide, 2-Hydroxyethyl disulfide, and hydrogen peroxide in formic acid (performic acid) is reported in Scheme 1.

The FT-IR spectrum of graphene oxide is displayed in Figure 1a in which the bands at wavenumbers higher than 3000 cm<sup>-1</sup> exhibited stretching vibrations of hydroxyl groups [32]. The vibrational bands at 2959 and 2825 cm<sup>-1</sup> belong to CH aliphatic groups [33]. The peak at 1722 cm<sup>-1</sup> shows the stretching vibration of the carbonyl of ketone [34], while the one at 1623 cm<sup>-1</sup> indicates the vibration of conjugated double bonds moieties [35]. The vibrational bands around 1177 cm<sup>-1</sup> demonstrate the etheric groups [36].

FT-IR spectrum of catalyst (Figure 1b) showed stretching vibration bands at 3329 cm<sup>-1</sup> and higher frequencies belonging to hydroxyl groups on graphene oxide and hydroxyl groups of sulfonic acid [37]. Stretching vibrational bands of phenolic and alcoholic hydroxyls emerged at 3329 cm<sup>-1</sup> [38]. Furthermore, stretching vibrational bands of aliphatic CH groups can be identified at 2927 and 2851 cm<sup>-1</sup> [39]. In addition, the stretching vibrations of

carbonyl groups of carboxylic acids and esters are detected at  $1726\text{ cm}^{-1}$  [40]. Moreover, stretching vibrations of conjugated double bonds appeared at  $1626\text{ cm}^{-1}$  [41]; while vibrational bands of carbon-carbon double bonds and the carboxylate of graphene oxide can be seen at  $1574\text{ cm}^{-1}$  [42]. Likewise, the bands at  $1439\text{ cm}^{-1}$  can be attributed to bending vibrations of  $\text{CH}_2$  groups [43]. Vibrational bands of S-OH of the sulfonic acid groups can be

identified at  $1241\text{ cm}^{-1}$  [44]. Moreover, stretching vibrational bands of the etheric C-O groups emerged at around 1311, 1241, and  $1089\text{ cm}^{-1}$  [45]. The vibrational bands at 1088, 1050, and  $950\text{ cm}^{-1}$  indicate the stretching vibrations of S=O in the sulfonic acid group [46]. According to the FT-IR spectra of graphene oxide and catalyst, the functionalization of the catalyst was improved with ethane sulfonic acid.



**Scheme 1.** Preparation of the catalyst

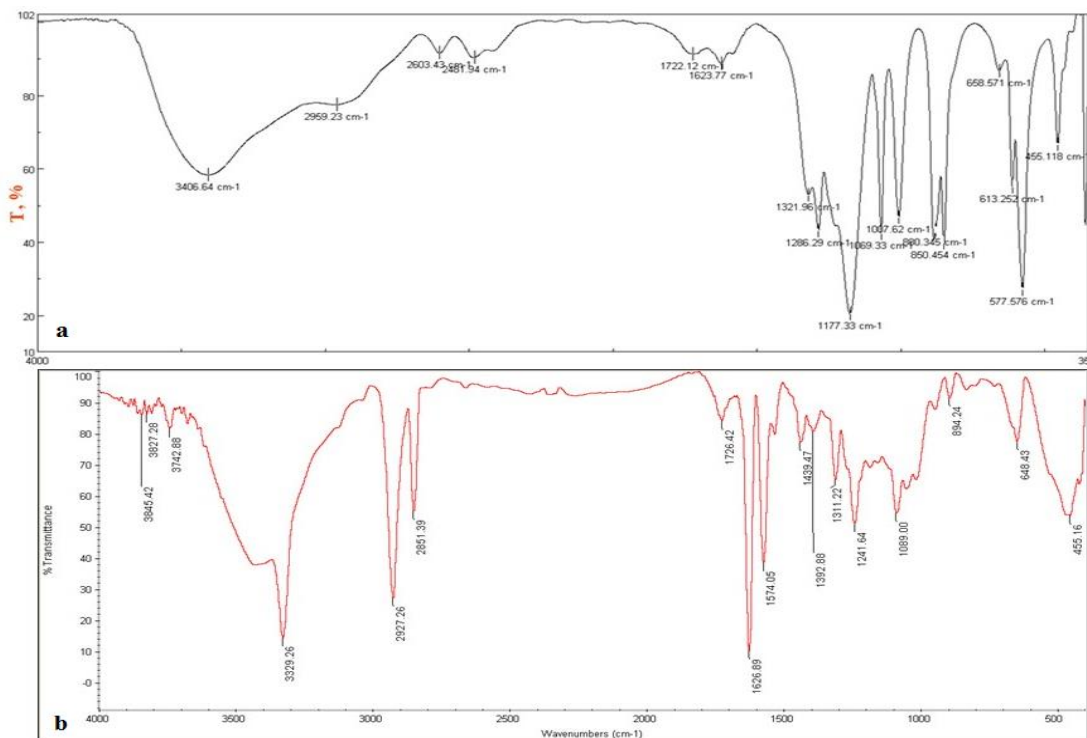


**Figure 1.** FT-IR spectra of a) GO and b) catalyst

The XRD spectra of graphene oxide, and catalyst are demonstrated in [Figure 2](#). XRD spectrum of graphene oxide showed a peak at  $2\theta = 11^\circ$  [47]. A broad and weak peak can be seen at  $2\theta = 18\text{-}20^\circ$  as a sign of the contaminant with reduced graphene oxide ([Figure 2a](#)). The XRD spectrum of the catalyst ([Figure 2b](#)) exhibited a broad peak at  $2\theta = 15\text{-}30^\circ$  belonging to non-crystalline nanostructured reduced graphene oxide [48], and the sharp peaks indicated the crystalline structures with various interlayer distances. According to XRD spectra of graphene oxide, and catalyst, the catalyst preparation increased the crystalline and nanostructured nature of graphene oxide.

The FE-SEM images of catalyst are represented in [Figure 3](#) which demonstrates flat and nanostructured layers.

The EDS analysis of catalyst is reported in [Figure 4](#). Based on the results, the catalyst showed the presence of carbon, oxygen, and sulfur on the surface, verifying the

functionalization of graphene oxide with ethane sulfonic acid.

Thermogravimetric analysis (TGA) of catalyst was carried out from 30 to 500 °C under an argon atmosphere ([Figure 5](#)). The diagram showed three steps weight loss. The first weight loss occurred at around 100 °C probably due to the solvents evaporation and physically adsorbed small molecules on the catalyst surface [49]. The second weight change occurred in the range of 175 to 210 °C probably due to the desorption of physically adsorbed molecules and dissociation of functional groups [50]. The third weight change was seen at 220 °C to 250 °C probably due to the destruction of the graphene oxide structure. According to the diagram, the total weight change and char yield were 55.41% and 44.59%, respectively. Thus, the catalyst is stable under reaction conditions and can be employed up to 200 °C without significant changes in its structure.



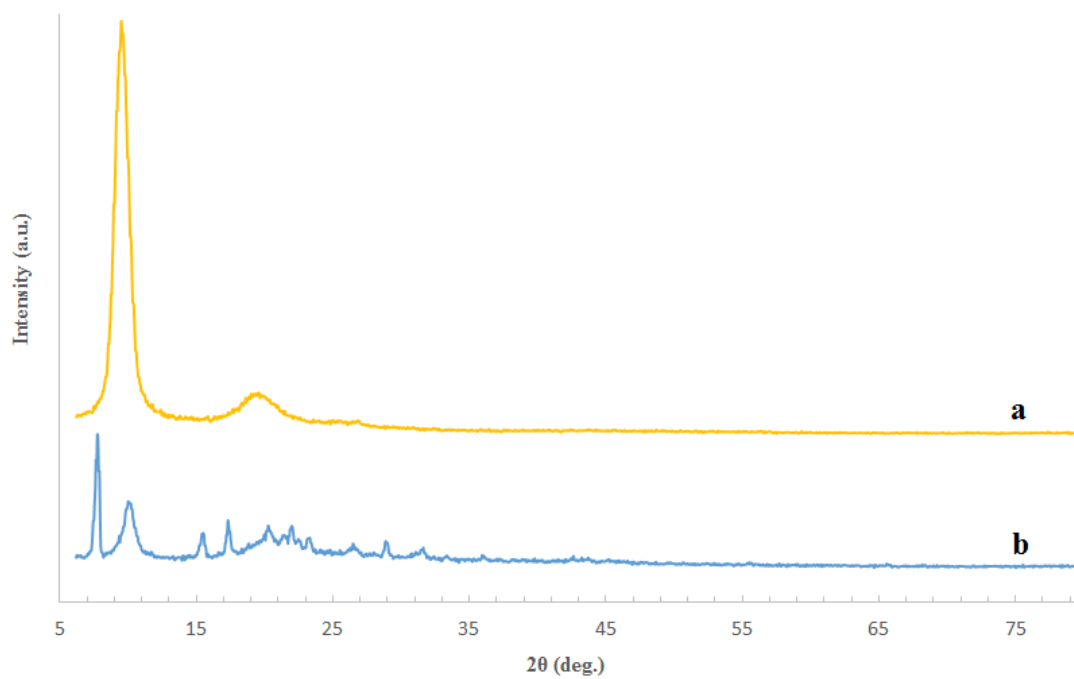


**Figure 2.** XRD patterns of a) GO, and b) catalyst

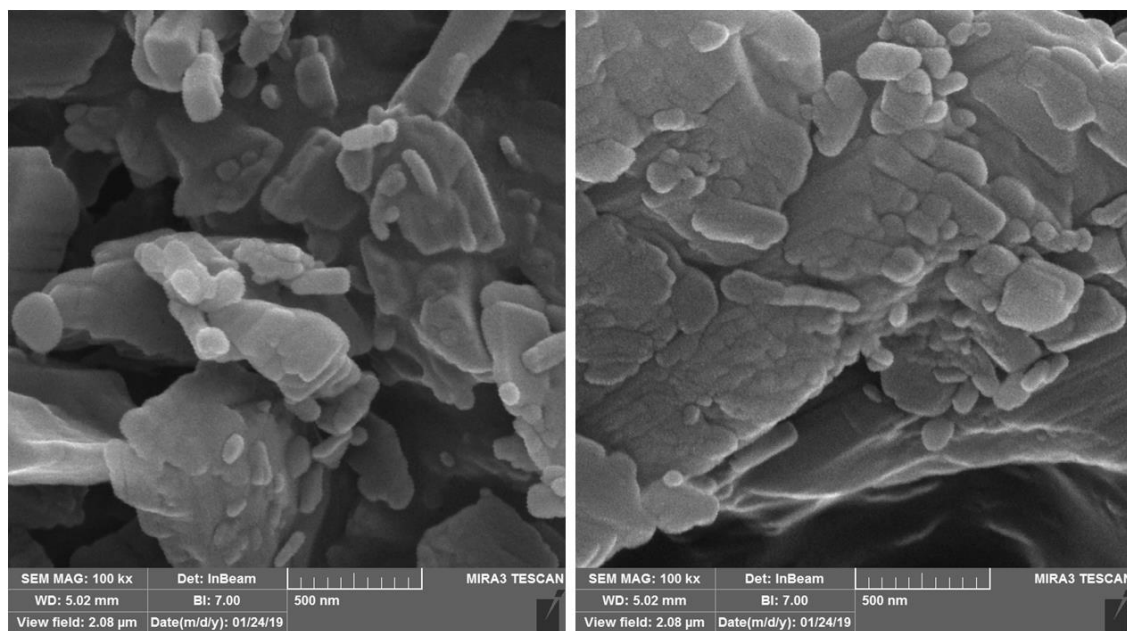


**Figure 3.** FE-SEM images of catalyst

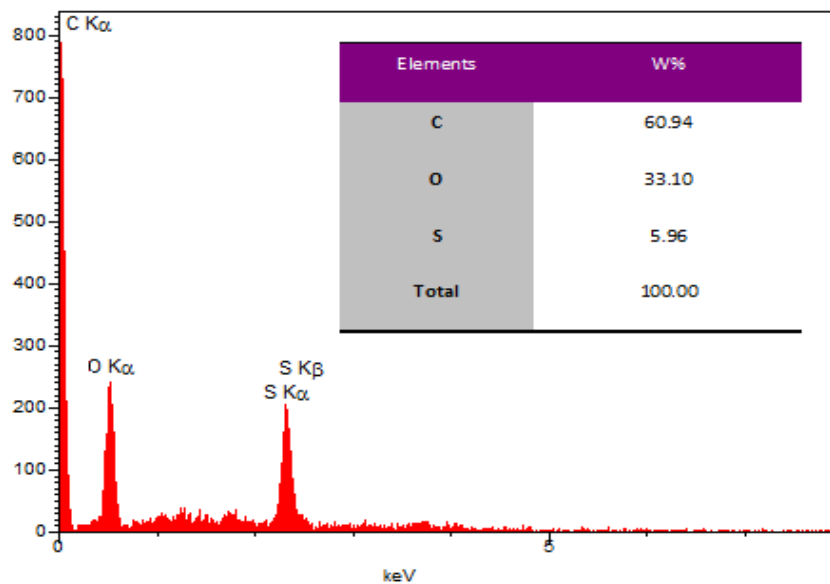


**Figure 4.** EDS analysis of catalyst

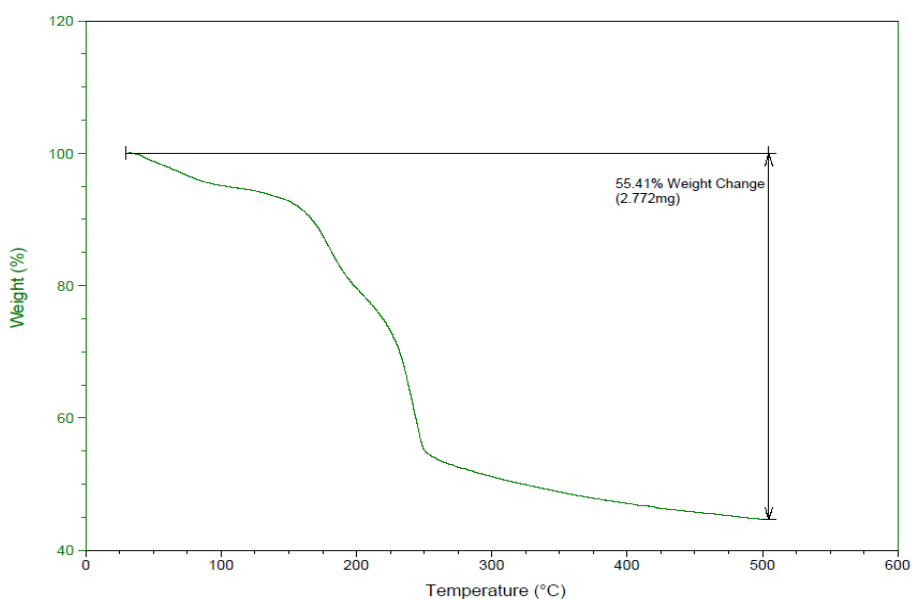


**Figure 5.** Thermogravimetric analysis (TGA) of catalyst

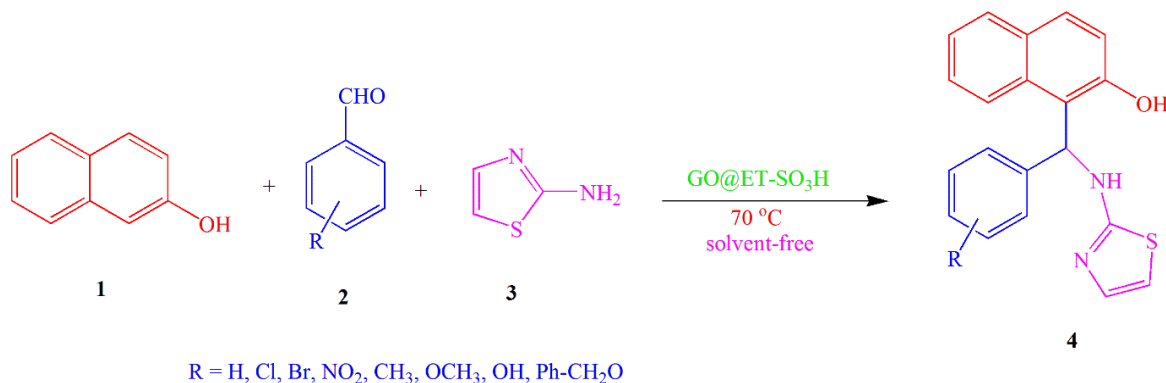
To examine the application of the developed catalyst in organic synthesis, the preparation of 1-[(1,3-thiazol-2-ylamino) methyl]-2-naphthols using 2-naphthol, aldehydes and 2-aminothiazole was studied. The optimum reaction conditions were determined during the preparation of **4b** by optimizing three variables including temperature, time, and

catalyst loading in solvent-free conditions (Scheme 2, Table 1). To 2-naphthol were added 3-nitrobenzaldehyde, 2-aminothiazole and catalyst (0.007 mol % based on sulfonic acid by using EDAX results) and mixed to afford a homogenized matrix. The reaction was performed in an oil bath and thin-layer chromatography (TLC) was employed to



monitor reaction progress using *n*-hexane and ethyl acetate (4:1). Ultimately, acetone was added to the reaction mixture and filtered. The filtrate was recrystallized in acetone to achieve

pure products. The recovery and reuse of the catalyst in the **4b** synthesis were examined by the reuse of the recovered catalyst five times and assessing the catalytic activity (Figure 6).



**Scheme 2.** Production of 1-[(1,3-thiazol-2-ylamino) methyl]-2-naphthols by using the catalyst

**Table 1.** Optimum conditions by using GO@ET-SO<sub>3</sub>H catalyst

Entry	Solvent	Catalyst (g)	Temperature (°C)	Time (min)	Yield (%) <sup>a</sup>
1	Solvent-free	-	25	180	71
2	Solvent-free	-	50	180	80
3	Solvent-free	0.01	50	40	78
4	Solvent-free	0.01	60	30	83
5	Solvent-free	0.02	60	30	89
6	Solvent-free	0.02	70	20	97
7	Solvent-free	0.02	80	20	97
8	Solvent-free	0.02	90	10	84
9	Solvent-free	0.03	70	20	95
10	Solvent-free	0.02 <sup>b</sup>	70	20	81

<sup>a</sup>Isolated yield

<sup>b</sup>GO

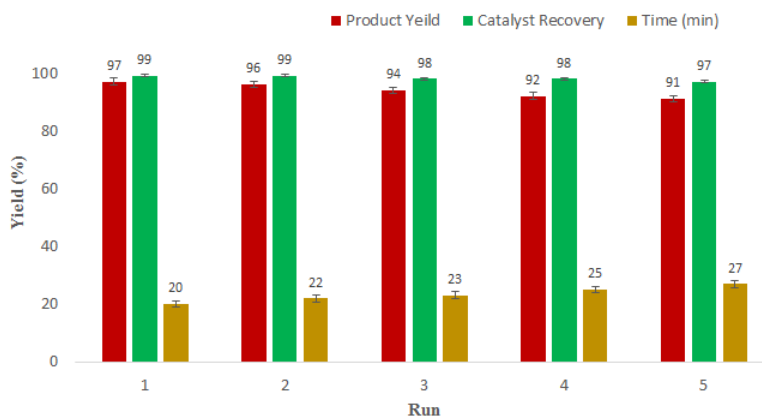


**Figure 6.** Catalyst recovery and reuse for preparing **4b** in five cycles

According to [Table 1](#), the best reaction conditions for the **4b** preparation (entry 6) involved solvent-free conditions, with 0.02 g of catalyst loading (0.007 mol % based on sulfonic acid), at 70 °C, for 20 min. The scope and limitations of the reaction were assessed by using aldehydes with various functional groups whose results are listed in [Table 2](#). The aldehydes products with electron-withdrawing functional groups and halogens showed higher yields compared with aldehydes by electron-donating functional groups [51].

#### Plausible mechanism of the reaction

The plausible reaction mechanism in the presence of the catalyst is depicted in [Scheme 3](#). Accordingly, aldehyde was initially activated by the catalyst (**I**), and then attacked by 2-naphthol (**II**) leading to intermediate **III** and **IV** [53]. After that, **IV** was protonated with catalyst (**V**), and water was omitted to afford intermediate **VI** [54]. Subsequently, **VI** was attacked by 2-

aminothiazole via 1,4-addition (Michael addition) through **VII** which was converted into the final products.

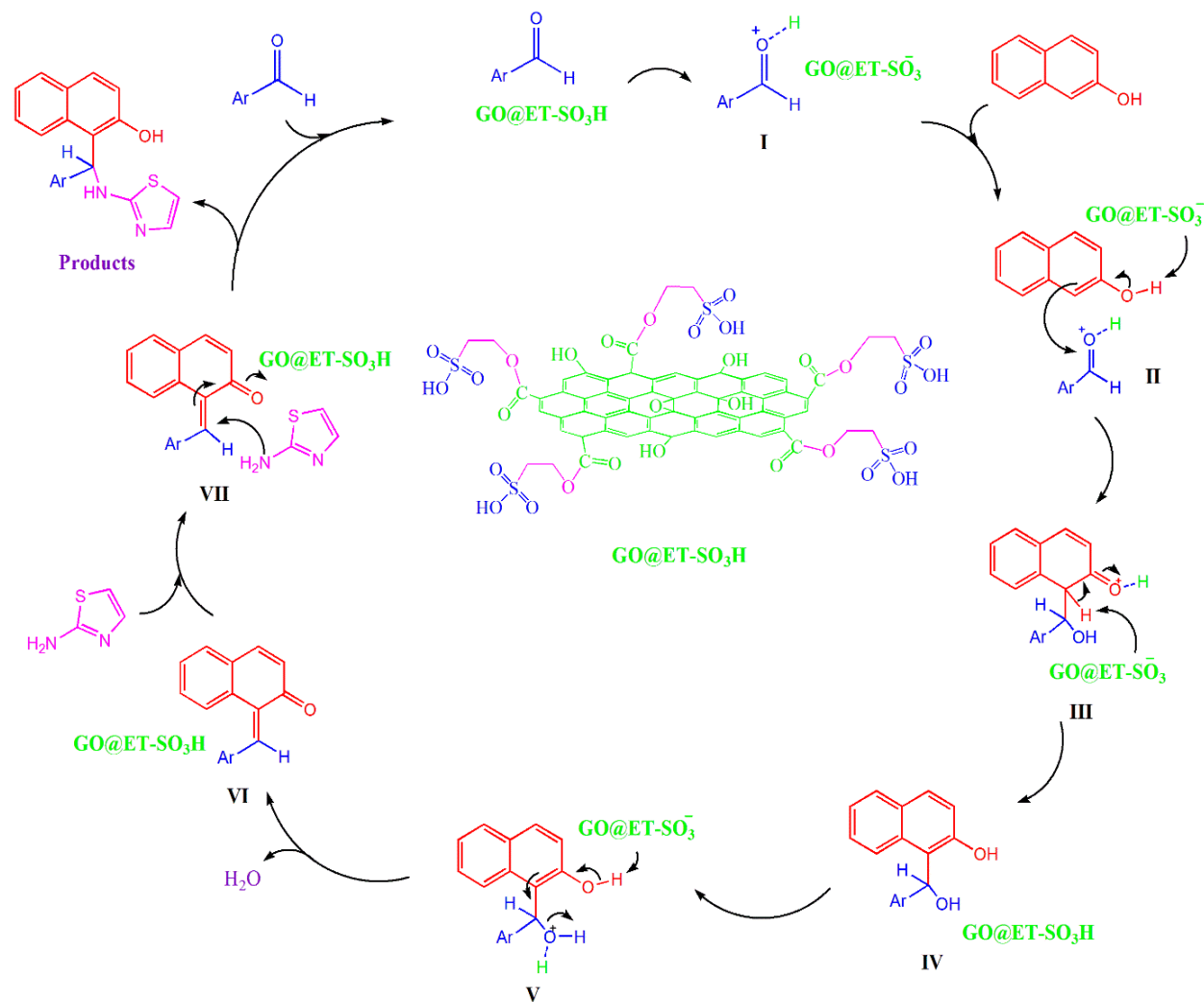
#### Catalyst recovery and reuse

The catalyst stability in the reaction condition and its reusability and recoverability in the **4b** synthesis were assessed after five times of recycling. Therefore, the catalyst was isolated and washed several times with ethyl acetate and dried and reused in the synthesis procedure ([Figure 6](#)). According to the diagram, after five times recovery, the catalyst stability in the reaction conditions showed no significant alterations. On the other hand, the product yields in these five times revealed no significant change, confirming the repeatability of catalytic activity and catalyst reproducibility. The catalyst yielded high values of turnover number (TON) and turnover frequency (TOF) for **4b** product in five runs ([Table 3](#)) [55].

**Table 2.** Synthesis of 1-[(1,3-thiazol-2-ylamino) methyl]-2-naphthols by using GO@ET-SO<sub>3</sub>H

Comp. no.	Ar	Time (min)	Yield <sup>a</sup> (%)	M.P. (°C)	
				Found	Reported [Lit.]
4a	C <sub>6</sub> H <sub>5</sub>	30	96	196-197	196-198 [52, 13]
4b	3-O <sub>2</sub> NC <sub>6</sub> H <sub>4</sub>	20	97	182-183	181-183 [52, 13]
4c	4-ClC <sub>6</sub> H <sub>4</sub>	20	97	171-172	170-171 [52]
4d	2-ClC <sub>6</sub> H <sub>4</sub>	30	95	178-179	180-182 [52]
4e	2,4-Cl <sub>2</sub> C <sub>6</sub> H <sub>3</sub>	20	96	165-166	164-166 [13]
4f	4-BrC <sub>6</sub> H <sub>4</sub>	25	94	174-175	173-175 [13]
4g	2-CH <sub>3</sub> OC <sub>6</sub> H <sub>4</sub>	40	92	151-152	152-154 [52]
4h	4-CH <sub>3</sub> OC <sub>6</sub> H <sub>4</sub>	30	94	160-161	158-160 [52]
4i	4-CH <sub>3</sub> C <sub>6</sub> H <sub>4</sub>	35	92	163-164	163-165 [13]
4j	4-OHC <sub>6</sub> H <sub>4</sub>	20	91	202-203	200-202 [52]
4k	C <sub>6</sub> H <sub>5</sub> CH <sub>2</sub> OC <sub>6</sub> H <sub>4</sub>	40	93	154-155	153-155 [13]

<sup>a</sup>Isolated yield



**Scheme 3.** Plausible mechanism for the synthesis of 1-[(1,3-thiazol-2-ylamino) methyl]-2-naphthols

**Table 3.** Recyclability, TON, and TOF values

Run	Time (min)	Yield <sup>a</sup> (%)	TON <sup>b</sup>	TOF (h <sup>-1</sup> ) <sup>c</sup>
1	20	97	13857	41571
2	22	96	13714	37401
3	23	94	13428	35029
4	25	92	13142	31540
5	27	91	13000	28888

<sup>a</sup>Isolated yield

<sup>b</sup>Turnover number

<sup>c</sup>Turnover frequency

## Conclusions

Graphene oxide functionalized ethane sulfonic acid was applied as an efficient and sustainable catalyst for the synthesis of 1-[(1,3-

Thiazol-2-ylamino) methyl]-2-naphthols under solvent-free conditions following the principles of green chemistry. The catalyst was prepared in two synthetic routes: first, graphene oxide was functionalized with 2-Hydroxyethyl

disulfide, and then the product was treated with hydrogen peroxide in formic acid. 1-[(1,3-thiazol-2-ylamino) methyl]-2-naphthols were synthesized via a one-pot three-component reaction of 2-naphthol, aromatic aldehydes and 2-aminothiazole in the presence of the prepared catalyst with high yields. The scope and limitations of the procedure were examined by using aromatic aldehydes with various functional groups. The functional groups had no significant effect on the product yields. The developed catalyst and applied procedure offered proper sustainability, short reaction time, solvent-free condition, availability, high TON and TOF values, and stability of the catalyst. Based on the above advantages, this catalyst can be efficiently utilized in chemistry and material science.

### Acknowledgments

The authors would like to appreciate Payam-e-Noor University (PNU) Research Council for supporting this research study.

### Disclosure Statement

No potential conflict of interest was reported by the authors.

### Funding

This research did not receive any specific grant from funding agencies in the public, commercial, or not-for-profit sectors.

### Authors' contributions

All authors contributed to data analysis, drafting, and revising of the paper and agreed to be responsible for all the aspects of this work.

### Orcid

Esmael Rostami  0000-0002-6512-9951

### References

- [1]. a) Iwanejko J., Wojaczyńska E., Olszewski T.K. *Curr. Opin. Green Sustain. Chem.*, 2018, **10**:27 [[Crossref](#)], [[Google Scholar](#)], [[Publisher](#)] b) Betti M. *Org. Synth. Collect.*, 1941, **1**:381 [[Crossref](#)], [[Google Scholar](#)], [[Publisher](#)] c) Betti M. *Gazz. Chim. Ital.*, 1900, **30**:301 [[Crossref](#)], [[Google Scholar](#)], [[Publisher](#)]
- [2]. Xu P.F., Wang W., eds., *Catalytic cascade reactions*. John Wiley & Sons, (2013) [[Crossref](#)], [[Google Scholar](#)], [[Publisher](#)]
- [3]. Kumar A., Gupta M.K., Kumar M. *ChemInform*, 2010, **41**:1582 [[Crossref](#)], [[Google Scholar](#)], [[Publisher](#)]
- [4]. Shen A.Y., Tsai C.T., Chen C.L. *Eur. J. Med. Chem.*, 1999, **34**:877 [[Crossref](#)], [[Google Scholar](#)], [[Publisher](#)]
- [5]. Szatmári I., Fülöp F. *Curr. Org. Synth.*, 2004, **1**:155 [[Crossref](#)], [[Google Scholar](#)], [[Publisher](#)]
- [6]. Shaterian H.R., Yarahmadi H. *Tetrahedron Lett.*, 2008, **49**:1297 [[Crossref](#)], [[Google Scholar](#)], [[Publisher](#)]
- [7]. Gao H., Sun J., Yan C.G. *Chin. Chem. Lett.*, 2015, **26**:353 [[Crossref](#)], [[Google Scholar](#)], [[Publisher](#)]
- [8]. Decottignies A., Len C., Fihri A. *Chemsuschem*, 2010, **5**:502 [[Crossref](#)], [[Google Scholar](#)], [[Publisher](#)]
- [9]. Azizi N., Edrisi M. *Res. Chem. Intermed.*, 2017, **43**:379 [[Crossref](#)], [[Google Scholar](#)], [[Publisher](#)]
- [10]. Rakhtshah J., Ghaderi H., Yaghoobi F., Baghery S., Shaabani B. *Mater. Chem. Phys.*, 2020, **239**:121985 [[Crossref](#)], [[Google Scholar](#)], [[Publisher](#)]
- [11]. Waghmode N.A., Kalbandhe A.H., Thorat P.B., Karade N.N. *Tetrahedron Lett.*, 2016, **57**:680 [[Crossref](#)], [[Google Scholar](#)], [[Publisher](#)]
- [12]. Rekunge D.S., Bendale H.S., Chaturbhuj G.U. *Monatsh. Chem.*, 2018, **149**:1991 [[Crossref](#)], [[Google Scholar](#)], [[Publisher](#)]

- [13]. Pelit E., Turgut Z. *J. Chem.*, 2016, **2016**:1 [[Crossref](#)], [[Google Scholar](#)], [[Publisher](#)]
- [14]. Kamali F., Shirini F. *Appl. Organomet. Chem.*, 2018, **32**:e3972 [[Crossref](#)], [[Google Scholar](#)], [[Publisher](#)]
- [15]. Adrom B., Maghsoodlou M.T., Hazeri N., Lashkari M. *Res. Chem. Intermed.*, 2015, **41**:7553 [[Crossref](#)], [[Google Scholar](#)], [[Publisher](#)]
- [16]. Maghsoodlou M.T., Karima M., Lashkari M., Adrom B., Aboonajmi J. *J. Iran. Chem. Soc.*, 2017, **14**:329 [[Crossref](#)], [[Google Scholar](#)], [[Publisher](#)]
- [17]. Shaterian H.R., Hosseinian A. *Sci. Iran*, 2014, **21**:727 [[Crossref](#)], [[Google Scholar](#)], [[Publisher](#)]
- [18]. Benzekri Z., Sibous S., Hsissou R., Boukhris S., Souizi A. *Chem. Data Collect.*, 2021, **31**:100599 [[Crossref](#)], [[Google Scholar](#)], [[Publisher](#)]
- [19]. Benzekri Z., Sibous S., Serrar H., Ouasri A., Boukhris S., Ghailane R., Rhandour A., Souizi A. *J. Mol. Struct.*, 2020, **1202**:127308 [[Crossref](#)], [[Google Scholar](#)], [[Publisher](#)]
- [20]. Lal J., Singh S., Rani P. *Chemistry Africa*, 2020, **3**:53 [[Crossref](#)], [[Google Scholar](#)], [[Publisher](#)]
- [21]. Afsharpour R., Zanganeh S., Kamantorki S., Fakhraei F. and Rostami E. *Asian J. Nanosci. Mater.*, 2020, **3**:148 [[Crossref](#)], [[Google Scholar](#)], [[Publisher](#)]
- [22]. Saryazdi F.H., Golrasan E., Heidari S. *Asian J. Green Chem.*, 2021, **5**:325 [[Crossref](#)], [[Google Scholar](#)], [[Publisher](#)]
- [23]. Hakimi F., Mirjalili F., Fallah-Mehrjardi M. *Asian J. Green Chem.*, 2020, **4**:183 [[Crossref](#)], [[Google Scholar](#)], [[Publisher](#)]
- [24]. Alem M., Kazemi S., Teimouri A., Salavati H. *Asian J. Green Chem.*, 2019, **3**:366 [[Crossref](#)], [[Google Scholar](#)], [[Publisher](#)]
- [25]. Yang G., Li L., Lee W.B., Ng M.C. *Sci. Technol. Adv. Mater.*, 2018, **19**:613 [[Crossref](#)], [[Google Scholar](#)], [[Publisher](#)]
- [26]. Ghosh P., Mukherji S. *Bioresour. Technol.*, 2021, **341**:125860 [[Crossref](#)], [[Google Scholar](#)], [[Publisher](#)]
- [27]. Rostami E., Kordrostami Z. *Asian J. Nanosci. Mater.*, 2020, **3**:203 [[Crossref](#)], [[Google Scholar](#)], [[Publisher](#)]
- [28]. Mohammadi R., Sabourmoghaddam N. *Asian J. Green Chem.*, 2020, **4**:11 [[Crossref](#)], [[Google Scholar](#)], [[Publisher](#)]
- [29]. Samadi N., Ansari R., Khodavirdilo B. *Asian J. Green Chem.*, 2018, **3**:288 [[Crossref](#)], [[Google Scholar](#)], [[Publisher](#)]
- [30]. Ebajo V.D., Santos C.R.L., Alea G.V., Lin Y.A., Chen C.H. *Sci. Rep.*, 2019 **9**:1 [[Crossref](#)], [[Google Scholar](#)], [[Publisher](#)]
- [31]. Alam S.N., Sharma N., Kumar L. *Graphene*, 2017, **6**:1 [[Crossref](#)], [[Google Scholar](#)], [[Publisher](#)]
- [32]. Ulaş Y. *J. Struct. Chem.*, 2021, **62**:356 [[Crossref](#)], [[Google Scholar](#)], [[Publisher](#)]
- [33]. Tugarova A.V., Mamchenkova P.V., Dyatlova Y.A., Kamnev A.A. *Spectrochim. Acta A Mol. Biomol. Spectrosc.*, 2018, **192**:458 [[Crossref](#)], [[Google Scholar](#)], [[Publisher](#)]
- [34]. Zhang C.H., Liu X.J., Zhang R., Tu Y. *Chin. J. Appl. Chem.*, 2021, **38**:271 [[Crossref](#)], [[Google Scholar](#)], [[Publisher](#)]
- [35]. Kumar V., Roy B.K. *Sci. Rep.*, 2018, **8**:1 [[Crossref](#)], [[Google Scholar](#)], [[Publisher](#)]
- [36]. Ahamad M.N., Iman K., Raza M.K., Kumar M., Ansari A., Ahmad M., Shahid M. *Bioorg. Chem.*, 2020, **95**:103561 [[Crossref](#)], [[Google Scholar](#)], [[Publisher](#)]
- [37]. Ali M., Mujtaba-ul-Hassan S., Ahmad J., Khurshid A., Shahzad F., Iqbal Z., Mehmood M., Waheed K. *Mater. Lett.*, 2019, **241**:23 [[Crossref](#)], [[Google Scholar](#)], [[Publisher](#)]
- [38]. Stalin N., Shobhanadevi N. *Biomass Convers. Biorefin.*, 2021, **1** [[Crossref](#)], [[Google Scholar](#)], [[Publisher](#)]
- [39]. Kumar M.M., Kumari S.B., Kavitha E., Velmurugan B., Karthikeyan S. *SN Appl. Sci.*,

- 2020, **2**:1 [Crossref], [Google Scholar], [Publisher]
- [40]. Herrera-Kao W.A., Loría-Bastarrachea M.I., Pérez-Padilla Y., Cauich-Rodríguez J.V., Vázquez-Torres H., Cervantes-Uc J.M. *Polym. Bull.*, 2018, **75**:4191 [Crossref], [Google Scholar], [Publisher]
- [41]. Kurbah S.D. *J. Coord. Chem.*, 2021, **74**:905 [Crossref], [Google Scholar], [Publisher]
- [42]. Geng S., Ren N., Zhang Y.Y., Tang K., Zhang J.J. *J. Solid State Chem.*, 2022, **305**:122633 [Crossref], [Google Scholar], [Publisher]
- [43]. Salehiabar M., Nosrati H., Javani E., Aliakbarzadeh F., Manjili H.K., Davaran S., Danafar H. *Int. J. Biol. Macromol.*, 2018, **115**:83 [Crossref], [Google Scholar], [Publisher]
- [44]. Periasamy A., Muruganand S., Palaniswamy M. *Rasayan J. Chem.*, 2009, **2**:981 [Crossref], [Google Scholar], [Publisher]
- [45]. Jiao L., Xiao H., Wang Q., Sun J. *Polym. Degrad. Stab.*, 2013, **98**:2687 [Crossref], [Google Scholar], [Publisher]
- [46]. Platero E.E., Mentrut M.P., Areán C.O., Zecchina A. *J. Catal.*, 1996, **162**:268 [Crossref], [Google Scholar], [Publisher]
- [47]. Esmaeili Y., Bidram E., Zarrabi A., Amini A., Cheng C. *Sci. Rep.*, 2020, **10**:1. [Crossref], [Google Scholar], [Publisher]
- [48]. Abbaspour S., Nourbakhsh A., Ebrahimi R., Ghayour H., Mackenzie K.J. *Mater. Sci. Eng. B*, 2019, **246**:89 [Crossref], [Google Scholar], [Publisher]
- [49]. Ndolomingo M.J., Meijboom R. *Appl. Catal. B: Environ.*, 2016, **199**:142 [Crossref], [Google Scholar], [Publisher]
- [50]. Abbasian M., Roudi M.M., Mahmoodzadeh F., Eskandani M., Jaymand M. *Int. J. Biol. Macromol.*, 2018, **118**:1871 [Crossref], [Google Scholar], [Publisher]
- [51]. DeváPegu C. *RSC advances*, 2016, **6**:40552 [Crossref], [Google Scholar], [Publisher]
- [52]. Li Z., Mao X. *Heterocycl. Commun.*, 2011, **17**:219 [Crossref], [Google Scholar], [Publisher]
- [53]. Hadadianpour E., Pouramiri B. *Molecular Diversity*, 2020, **24**:241 [Crossref], [Google Scholar], [Publisher]
- [54]. Mansouri M., Habibi D., Heydari S. *Res. Chem. Intermed.*, 2022, **48**:683 [Crossref], [Google Scholar], [Publisher]
- [55]. Mondal S., Singh J., Singh S., Vishwakarma S., Mitra K., Kumari A., Singh R., Gupta S.K.S., Ray B. *New J. Chem.*, 2020, **44**:10878 [Crossref], [Google Scholar], [Publisher]

**How to cite this manuscript:** Samaneh Hamidi Zare, Maryam Sadat Ghorayshi Nejad, Ali Saberi, Esmael Rostami\*. A highly efficient and sustainable synthesis of 1-[(1,3-thiazol-2-ylamino) methyl]-2-naphthols under solvent-free conditions using graphene oxide substituted ethane sulfonic acid catalyst. *Asian Journal of Nanoscience and Materials*, 5(3) 2022, 211-224. DOI: 10.26655/AJNANOMAT.2022.3.4